Vol 17 No 3, March 2008
1674-1056/2008/17(03)/1020-05

Chinese Physics B

© 2008 Chin. Phys. Soc.
and IOP Publishing Ltd

Photonic crystal fibre Brillouin laser based on Bragg grating Fabry–Perot cavity*

Geng Dan(耿 丹), Yang Dong-Xiao(杨冬晓)†,
Shen Guo-Feng(沈国锋), and Zhang Xian-Min(章献民)

Department of Information & Electronic Engineering, Zhejiang University, Hangzhou 310027*, China*

(Received 19 March 2007; revised manuscript received 13 April 2007)

A photonic crystal fibre Brillouin laser based on fibre Bragg grating Fabry–Perot cavity is presented. A highly nonlinear photonic crystal fibre 25 m in length is used as Brillouin gain medium and fibre Bragg grating Fabry–Perot cavity is chosen in order to enhance the laser conversion efficiency and suppress the higher-order Stokes waves. The laser reaches the threshold at input power of 35 mW, and the experimental laser conversion efficiency achieves 18% of the input power of 140 mW and does not show higher-order Stokes waves. A photonic crystal fibre Brillouin laser with shorter fibre length and lower threshold is experimentally realized.

Keywords: photonic crystal fibre, two-frequency laser, stimulated Brillouin scattering
PACC: 4270Q, 4255N, 4265C

1. Introduction

Photonic crystal fibre (PCF) technology has been progressing rapidly in recent years.[1,2] PCF combines small core area with single-mode behaviour over a wide wavelength range.[3] A number of research groups have studied nonlinear effects in PCF and demonstrated a variety of results, such as the generation of a supercontinuum,[4,5] all-optical switch,[6] Raman amplifiers,[7] four-wave mixing,[3] and Brillouin laser.[8,9] In Ref.[8], a holey fibre Brillouin laser has been demonstrated comprising a high-reflectivity mirror cavity with 73.5 m of holey fibre, which reached the threshold at a pump power of 125 mW. A Brillouin laser in the ring cavity configuration has been presented.[9] This laser with 100 m of holey fibre reached the threshold at a pump power of 63 mW, and tends to produced high-order Stokes waves.

According to Randoux's research, stability of the stimulated Brillouin scattering is affected by fibre length in the fibre ring and fibre resonance cavity. Only when the fibre length is short enough, stable Brillouin scattering output of fibre laser with arbitrary pump wave input can be achieved.[10] Theoretically, Fabry–Perot (FP) cavity using fibre grating pair may have arbitrary cavity length, therefore, stable Brillouin scattering output may be realized using fibre grating FP cavity.

Recently, two-frequency Brillouin fibre lasers have attracted considerable attentions. They have many applications such as all-optical 2R regeneration, microwave generation and microwave photonics conversion.[11,12] In this paper, we present a PCF two-frequency Brillouin laser based on fibre Bragg grating (FBG) pair as FP cavity along with 25-m PCF as the Brillouin gain medium. The laser reached threshold at a input power of 35 mW. A PCF Brillouin laser with shorter fibre length and higher conversion efficiency was experimentally realized.

2. Theoretical analysis

The laser cavity consists of a fibre FP cavity closed by two FBGs. In our scheme, the appearance of the higher-order Stokes waves can be avoided by selecting proper FBGs and tuning their reflectivity spectra. A FBG with narrow bandwidth (narrower than Brillouin frequency shift ν_{B}) was chose as FBG1 as shown in Fig.1.

*Project supported by the National Natural Science Foundation of China (Grant Nos 60577028, 60407011 and 60177025) and the Research Fund for the Doctoral Program of Higher Education, China.
†Corresponding author. E-mail: yangdx@zju.edu.cn

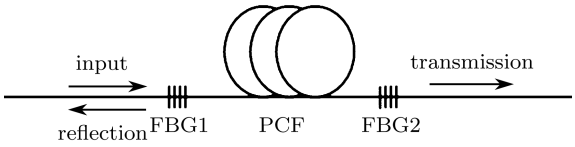


Fig.1. Schematic setup of the PCF Brillouin laser based on fibre Bragg grating Fabry–Perot cavity.

Its central reflection frequency was tuned to Stokes frequency. Since the bandwidth of FBG1 is narrower than ν_{B}, the reflectivity of FBG1 at the wavelength of the higher-order Stokes wave and pump wave is very low, therefore, the pump wave can easily enter into the fibre FP cavity and the appearance of the higher-order Stokes waves can then be avoided. We chose the other FBG with relatively wide bandwidth (wider than $2\nu_{\mathrm{B}}$) as FBG2 in Fig.1, which assures that the pump wave and Stokes wave can be reflected effectively, and its central reflection frequency is tuned to the pump frequency. Generated Stokes wave is amplified along its each path in the cavity. Neglecting phase of each wave in the coupled-amplitude equations, we obtain the following coupled-power equations.[13–15]

$$\partial P_{\mathrm{P}}^{+}/\partial z = -\alpha P_{\mathrm{P}}^{+}(z) - g_{\mathrm{B}} P_{\mathrm{P}}^{+}(z) P_{\mathrm{S}}^{-}(z)/A_{\mathrm{eff}}, \quad (1)$$

$$\partial P_{\mathrm{S}}^{-}/\partial z = \alpha P_{\mathrm{S}}^{-}(z) - g_{\mathrm{B}} P_{\mathrm{P}}^{+}(z) P_{\mathrm{S}}^{-}(z)/A_{\mathrm{eff}}, \quad (2)$$

$$\partial P_{\mathrm{P}}^{-}/\partial z = \alpha P_{\mathrm{P}}^{-}(z) + g_{\mathrm{B}} P_{\mathrm{P}}^{-}(z) P_{\mathrm{S}}^{+}(z)/A_{\mathrm{eff}}, \quad (3)$$

$$\partial P_{\mathrm{S}}^{+}/\partial z = -\alpha P_{\mathrm{S}}^{+}(z) + g_{\mathrm{B}} P_{\mathrm{P}}^{-}(z) P_{\mathrm{S}}^{+}(z)/A_{\mathrm{eff}}, \quad (4)$$

where $P_{\mathrm{P}}(z)$ and $P_{\mathrm{S}}(z)$ are the powers of pump and the Stokes waves, respectively. The superscripts $+/-$ represent the direction of propagation. g_{B} is the Brillouin gain coefficient of the fibre and α is the attenuation coefficient. A_{eff} is the effective core area of the fibre. The boundary conditions at the input ($z = 0$) and output ($z = L$) FBG are given by

$$P_{\mathrm{P}}^{+}(0) = (1 - R_{\mathrm{P0}}) P_{\mathrm{in}} + R_{\mathrm{P0}} P_{\mathrm{P}}^{-}(0), \quad (5)$$

$$P_{\mathrm{S}}^{+}(0) = R_{\mathrm{S0}} P_{\mathrm{S}}^{-}(0), \quad (6)$$

$$P_{\mathrm{P}}^{-}(L) = R_{\mathrm{PL}} P_{\mathrm{P}}^{+}(L), \quad (7)$$

$$P_{\mathrm{S}}^{-}(L) = R_{\mathrm{SL}} P_{\mathrm{S}}^{+}(L), \quad (8)$$

where R_{P0} and R_{S0} are the reflectivities of FBG1 at the wavelengths of the pump wave and Stokes wave, respectively. R_{PL} and R_{SL} are the reflectivities of FBG2 at the wavelengths of the pump waves and Stokes wave, respectively. P_{in} is the input power and $(1–R_{\mathrm{P0}})P_{\mathrm{in}}$ is the pump power injected into the cavity. The output power of Stokes wave is

$$P_{\mathrm{Sout}} = P_{\mathrm{S}}^{-}(0)(1 - R_{\mathrm{S0}}). \quad (9)$$

When the input power P_{in} is given, we can obtain the conversion efficiency of the Brillouin laser as $\eta = P_{\mathrm{Sout}}/P_{\mathrm{in}}$. Figure 2 shows the relationship between theoretical conversion efficiency and input power. Here, the parameters for calculation are chosen as follows: Brillouin gain coefficient g_{B} is 5×10^{-11} m/W,[9] effective area of optical fibre A_{eff} is $10\,\mu\mathrm{m}^2$, the length of optical fibre is 25 m, fibre attenuation coefficient α is 9 dB/km, and the reflectivities of FBGs are $R_{\mathrm{S0}} = 0.417$, $R_{\mathrm{P0}} = 0.113$, $R_{\mathrm{SL}} = 0.959$ and $R_{\mathrm{PL}} = 0.977$, respectively. It is clear that conversion efficiency increases with the enhancement of input power. In practice, fibre splice loss and Bragg grating losses should reduce this conversion efficiency.

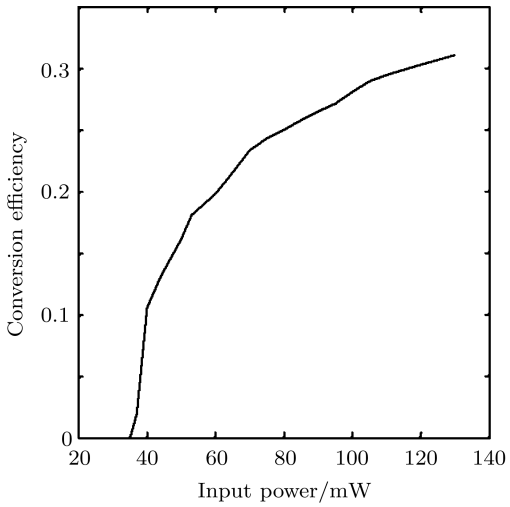


Fig.2. Variation of the theoretical conversion efficient with input power.

3. Experiment and results

The threshold of the first Brillouin Stokes wave in the single-pass regime was investigated firstly. The experimental setup is shown in Fig.3, and the FBG1 and the FBG2 were removed to avoid feedback from them in the experiment. The pump source is based on a tunable laser followed by Er doped fibre amplifier (EDFA). The linewidth of the tunable laser is 100 kHz. The circulator is used to launch the pump into the PCF and extract the Stokes wave. The geometry of the PCF is shown in the inset of Fig.3. It has a core diameter of 2.1 μm and has a model field diameter of 2.8 μm, and a loss of < 9 dB/km at 1510–1620 nm. The nonlinear coefficient of PCF is about

11 $(\mathrm{W}\cdot\mathrm{km})^{-1}$ at 1550 nm. 25-m PCF is used as Brillouin gain medium. Its Brillouin frequency shift is about 10.88 GHz. We experimentally observed a SBS threshold of 148 mW, as shown in Fig.4. Theoretically, the SBS threshold can be approximated by the following equation:[16]

$$P_{\mathrm{th}} = (21 \times A_{\mathrm{eff}})/(g_{\mathrm{B}} \times L_{\mathrm{eff}}), \tag{10}$$

where P_{th} is the SBS threshold, and L_{eff} is the effective fibre length:

$$L_{\mathrm{eff}} = [1 - \exp(-\alpha L)]/\alpha, \tag{11}$$

where L is fibre length. It is estimated from analytical equations (10) that the Brillouin threshold would be reached at a pump power of 143 mW, assuming a Brillouin gain coefficient of 5×10^{-11} m/W for the holey fibre and taking into account of the fibre parameters quoted above.[9]

We next investigated the performance of the fibre under laser operation. The experimental setup is shown in Fig.3. A polarization controller (PC) before FBG1 is used to control the polarization of the input pump wave. The second PC in fibre F–P cavity is used to adjust the polarization of Stokes wave to get maximum amplification. The reflection spectra of two FBGs used in the experiment are shown in Fig.5.

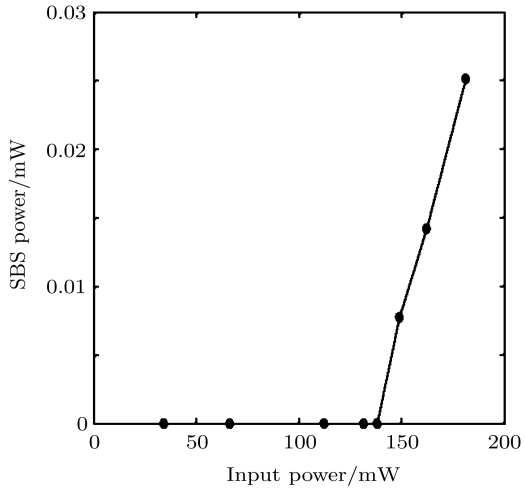


Fig.3. SBS (backward) versus input power.

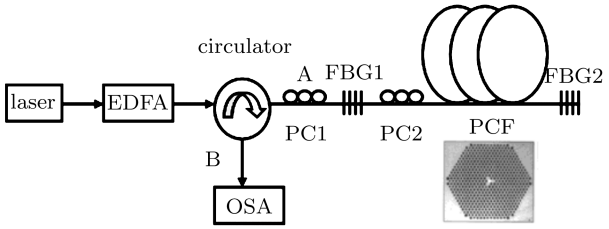
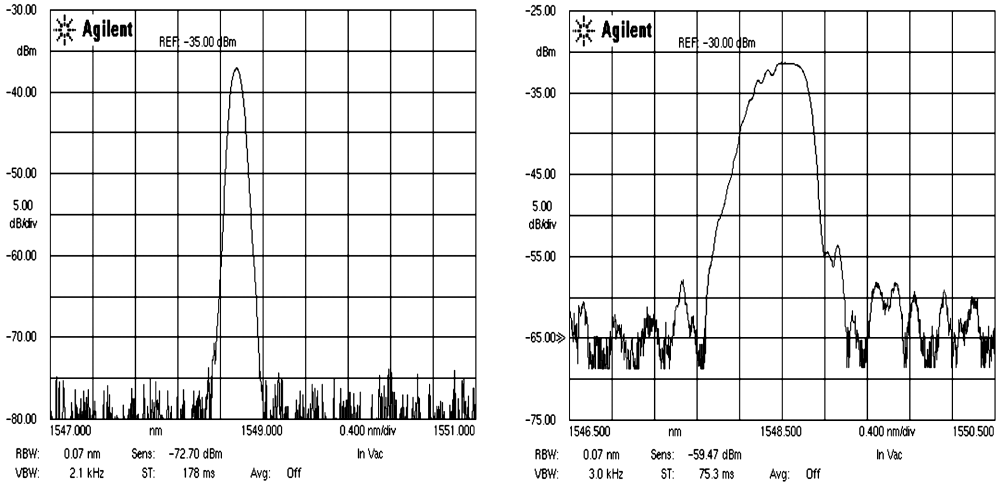


Fig.4. Experimental setup for two-frequency Brillouin fibre laser.



(a) FBG1 (b) FBG2

Fig.5. Reflection spectra of the two FBGs used in the Brillouin fibre laser.

The 3-dB bandwidths of FBG1 and FBG2 are 0.116 nm and 0.49 nm, respectively, and the reflectivities of FBGs are $R_{\mathrm{S0}} = 0.417$, $R_{\mathrm{P0}} = 0.113$, $R_{\mathrm{SL}} = 0.959$ and $R_{\mathrm{PL}} = 0.977$, respectively. By stretching the FBGs, their centre wavelengths can be tuned to the wavelength of Stokes wave. In this experiment, the wavelength of pump wave was set to 1548.68 nm, and the Stokes wave at the wavelength of 1548.76 nm was found. Figure 6 shows experimental data of the Brillouin laser output power (at B end) as a function

of the input power (at A end). Before laser threshold was reached, output Stokes power remained zero, while with input power increasing the output pump power increased. After laser threshold was reached, when input power further increased, the pump power was converted to Stokes power, so the output Stokes power rose promptly, and the output pump power decreased accordingly.

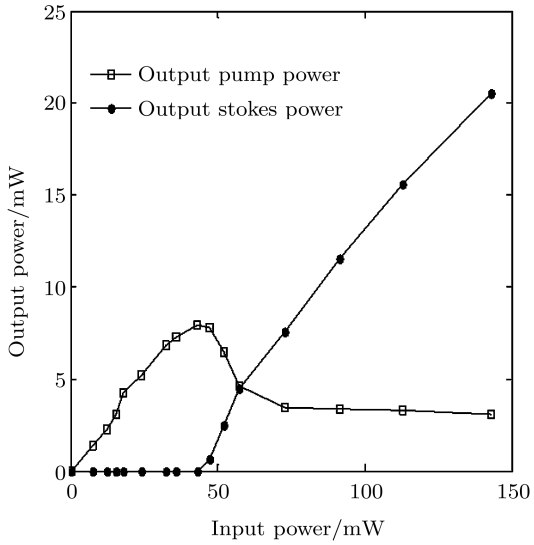


Fig.6. Laser output.

Figure 7 shows the relationship between experimental conversion efficiency and input power. The experimental threshold of the Brillouin laser was 35 mW, and it was estimated from equations (1–8) that Brillouin threshold would be reached at an input power of 35 mW. It is clear that conversion efficiency of the laser increases with the enhancement of input power, and the laser conversion efficiency achieves 18% for input power of 140 mW. Experimental conversion efficiency was less than the theoretical conversion efficiency. It is believed that the low conversion efficiency determined experimentally arises from axial fluctuations in the holey fibre cross-sectional profile which lowers the effective gain coefficient,[8] and the loss of FBGs and fibre splice loss also lower the conversion efficiency. The output optical spectrum of the Brillouin laser at input power of 57 mW is shown in Fig.8. The pump wave intensity and Stokes wave intensity are approximately equal. In the experiment, we have not observed the higher-order Stokes waves even when the input power increases to a very high level.

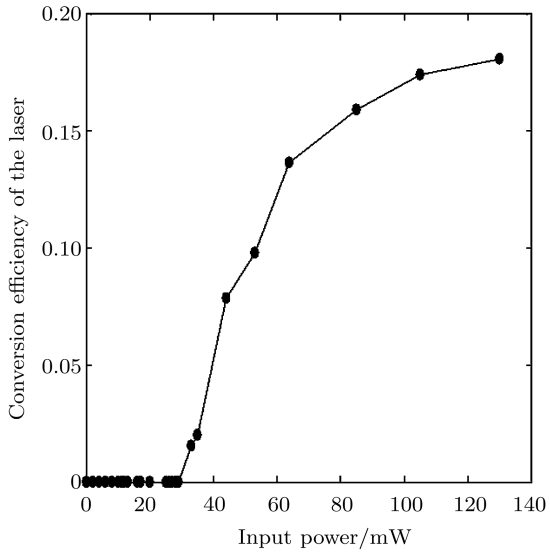


Fig.7. Variation of the conversion efficient with input power.

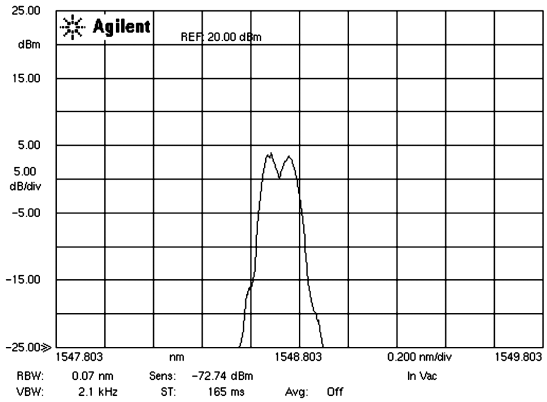


Fig.8. The output optical spectrum of the Brillouin laser at input power of 57 mW.

In conclusion, we have experimentally demonstrated a PCF Brillouin laser based on fibre Bragg grating Fabry–Perot cavity. 25-m PCF was used as Brillouin gain medium. The laser reached threshold at a input power of 35 mW. The experimental conversion efficiency achieved 18% for an input power of 140 mW, without showing the appearance of higher-order Stokes waves. A PCF Brillouin laser with shorter fibre length and lower threshold was also experimentally realized.

4. Acknowledgments

The authors thank Chi H for supplying photonic crystal fibre, and Xie H for helpful discussion.

References

[1] Liu X Y, Zhang F D, Zhang M and Ye P D 2007 *Acta Phys. Sin.* **56** 301 (in Chinese)

[2] Han Y, Hou L T, Hu M L, Li S G, Li Y F, Wang Q Y, Xing G L and Zhou G Y 2006 *Chin. Phys.* **15** 437

[3] Sharping J E, Fiorentino M, Coker A and Kumar P 2001 *Opt. Lett.* **26** 1048

[4] Hu M L, Wang Q Y, Li Y F, Wang Z, Zhang Z G, Chai L and Zhang R B 2004 *Acta Phys. Sin.* **53** 4243 (in Chinese)

[5] Jia Y Q, Yan P G, Lv K C, Zhang T Q and Zhu X N 2006 *Acta Phys. Sin.* **55** 1809 (in Chinese)

[6] Liu J G, Kai G Y, Xue L F, Zhang C S, Liu Y G, Wang Z, Guo H L, Li Y, Sun T T, Yuan S Z and Dong X Y 2007 *Acta Phys. Sin.* **56** 941 (in Chinese)

[7] Yusoff Z, Lee J H, Belardi W, Monro T M, Teh P C and Richardson D J 2002 *Opt. Lett.* **27** 424

[8] Lee J H, Yusoff Z, Belardi W, Ibsen M, Monro T M and Richardon D J 2002 *Opt. Lett.* **27** 927

[9] Matos C J S de, Taylor J R and Hansen K P 2004 *Opt. Commun.* **238** 185

[10] Randoux S, Lecoeuche V and Segard B 1995 *Phys. Rev.* A **51** 4345

[11] Shen Y C, Zhang X M and Chen K S 2005 *IEEE J. Lightwave Technology* **23** 1860

[12] Shen Y C, Jin X F, Zhang X M and Chen K S 2005 *Fibre and Integrated Optics* **24** 83

[13] Ogusu K 2002 *IEEE Photon. Technol. Lett.* **14** 947

[14] Randoux S, Lecoeuche V, Segard B and Zemmouri J 1995 *Phys. Rev.* A **52** 2327

[15] Ogusu K and Sakai A 2002 *Appl. Phys.* **41** 609

[16] Smith R G 1972 *Appl. Opt.* **11** 2489